Coexisting single-particle solutions in low-density symmetric nuclear matter

H. F. Arellano[*]
Department of Physics-FCFM, University of Chile, Santiago, Chile.
E-mail: `arellano@dfi.uchile.cl`

J.-P. Delaroche
CEA, DAM, DIF, F-91297 Arpajon, France.
E-mail: jean-paul.delaroche@cea.fr

Arnau Rios
Department of Physics, Faculty of Engineering and Physical Sciences, University of Surrey,
Guildford, Surrey GU2 7XH, United Kingdom
E-mail: a.rios@surrey.ac.uk

The only two-nucleon bound state system occurring in free space is the deuteron, constituted by a proton-neutron pair. Although the neutron-neutron interaction is attractive, its strength is not deep enough to allow for a bound state in the form of a dineutron. However, this picture changes drastically when the interacting neutrons are immersed in nuclear matter. In this contribution we address dinucleon properties as implied by the Brueckner-Hartree-Fock approximation for infinite symmetric nuclear matter at zero ($T = 0$) and finite temperature. Special emphasis is given to dinucleon formation in the search of self-consistent single-particle fields, leading to novel features for low-density nuclear matter, i.e. mass densities of the order of 10^{11-12} g cm^{-3}. Searches have been carried out at Fermi momenta in the range $0 < k_F \leq 1.75$ fm^{-1} using the Argonne v_{18} bare nucleon-nucleon potential. At $T = 0$, two distinct solutions meeting self-consistency are found with overlapping domains in the interval 0.130 fm$^{-1} \leq k_F \leq 0.285$ fm^{-1}. Effective masses as high as three times the nucleon mass are found in the coexistence domain, in resemblance to Heavy Fermions in strongly correlated systems. Self-consistent solutions for the single-particle fields at finite temperature are also investigated and preliminary results shall be presented.

---

[*]Speaker.

---

1. Introduction

The Brueckner, Bethe and Goldstone (BBG) theory for interacting nucleons has played an important role in the quest for a unified description of nuclear many-body phenomena based on the bare interaction between nucleons [1, 2]. At negative energies in the Brueckner-Hartree-Fock (BHF) approximation it has been extensively applied to the study of saturation properties of nuclear matter, including the equation of state over the whole range of isospin-asymmetry. At positive energies, as in the case of nucleon scattering from nuclei, the g matrix in the BHF approximation has been used to model density-dependent effective interactions between the projectile and target nucleons [3, 4].

Nuclear matter properties have been investigated within various frameworks such as microscopic quantum statistical approach and generalized relativistic mean field models [5], self-consistent Green's function theory [6, 7], quasiparticle gas models for the study of light nuclei in supernova envelopes [8], among many others. However, there is no retrievable reference known to these authors where dinucleon bound state correlations are explicitly treated, *in conjunction with* the self-consistent search of single-particle (sp) fields within the BHF approximation, particularly at very low densities. In this work we address this issue by providing an explicit account for dinucleon bound states in the $^1S_0$ and $^3S_1-^3D_1$ channels, expressed as isolated poles on the real axis below the continuum threshold, while seeking self-consistency within the continuous choice.

2. Framework

In BBG theory for symmetric nuclear matter the g matrix depends on the density of the medium, characterized by the Fermi momentum k_F, and starting energy ω [2]. To lowest order in the BHF approximation, when only two-body correlations are taken into account, the g matrix satisfies

$$g(\omega) = v + v \frac{Q}{\omega + i\eta - \hat{h}_1 - \hat{h}_2} g(\omega), \tag{2.1}$$

with v the bare interaction between nucleons, $\hat{h}_1(\hat{h}_2)$ the sp energy of nucleon $1(2)$, and Q the Pauli blocking operator. The solution to this equation enables the evaluation of the mass operator

$$M(k;E) = \sum_{|\mathbf{p}|\leq k_F} \langle \tfrac{1}{2}(\mathbf{k}-\mathbf{p})|g_{\mathbf{K}}(E+e_p)|\tfrac{1}{2}(\mathbf{k}-\mathbf{p})\rangle, \tag{2.2}$$

where $\mathbf{K}$ is the total momentum of the interacting pair, $\mathbf{K} = \mathbf{k} + \mathbf{p}$, and

$$e_p = \frac{p^2}{2m} + U(p), \tag{2.3}$$

the sp energy defined in terms of an auxiliary field U. The nucleon mass m is taken as the average of proton and neutron masses. In the BHF approximation the sp potential is given by the on-shell mass operator,

$$U(k) = \Re e\, M(k; e_k), \tag{2.4}$$

a self-consistency requirement which can only be achieved iteratively. In the continuous choice this condition is imposed to all momenta k [2].

A standard procedure to solve the non-linear system of Eqs. (2.1-2.4) is by iterative feed-backing, where the auxiliary field U is initially unknown. Cycles begin with a tentative guess for $U(k)$, which allows a solution for g from Eq. (2.1) for the specified values of ω and K. The series of cycles can be started with $U_0(k) = 0$, to obtain all g-matrix elements needed for the evaluation of M in Eq. (2.2). The real part of M defines a new sp field, U_1, which becomes the guess for a new cycle. The procedure is iterated until differences between consecutive solutions for U meet some convergence criterion. Although this self-consistent scheme works well at normal densities, convergence may become extremely difficult –if not unfeasible– as k_F diminishes below ~ 0.8 fm^{-1}. In this low-density regime, instabilities develop in the evaluation of the on-shell mass operator. We have noted that self-consistency at low densities can be reached by diminishing the number of mesh points for the Fermi-motion integral in Eq. (2.2). With this numerical compromise it is possible to avoid sudden fluctuations of the integrands, but the actual convergence of the integrals becomes dubious.

Aiming to obtain reliable self-consistent solutions for the sp mean fields over a wide density regime as well as accounting explicitly for dinucleon bound states, a refinement of numerical techniques becomes crucial to control instabilities during the iterative process. The evaluation of the sp fields, $U(k) = \Re e\, M(k, e_k)$, involves the summation of on-shell g-matrix elements while keeping the momentum of one of the particles below the Fermi surface. Explicitly,

$$M(k, e_k) = \sum_{\alpha} n_\alpha \int_0^{k_F} p^2 dp \int_{-1}^{1} du\, g_{\mathbf{k}+\mathbf{p}}^\alpha \left(\frac{|\mathbf{k}-\mathbf{p}|}{2}, \frac{|\mathbf{k}-\mathbf{p}|}{2}; \omega \right) . \tag{2.5}$$

Here $u = \hat{\mathbf{k}} \cdot \hat{\mathbf{p}}$, the energy ω is evaluated on-shell ($\omega = e_k + e_p$), α denotes spin, isospin and angular momentum states, and n_α accounts for their degeneracy and for geometric factors.

For most NN states the above integral involves well behaved integrands. However, extra measures becomes much needed for the $^1S_0$ and $^3S_1-^3D_1$ states. This is because during the evaluation of the momentum integral in Eq. (2.5), exceedingly large g-matrix elements stemming from NN bound states in these S and D channels do appear. Such bound states occur when

$$\det[1 - v_\alpha \Lambda_K(\omega)] = 0 , \tag{2.6}$$

where $\Lambda_K(\omega)$ denotes the particle-particle propagator in Eq. (2.1) and v_α denotes the bare potential in a particular NN channel. Any matrix element with starting energy ω and total momentum K near such bound states will lead to large contributions. In actual calculations these singularities can be controlled with the regularization

$$g(\omega) \to g(\omega) \times \frac{(\Delta\omega)^2}{(\Delta\omega)^2 + \eta^2} ,$$

where $\Delta\omega = \omega - \omega_K^*$. ω_K^* is the starting energy corresponding to a bound state of total momentum K, and η is reasonably small real parameter. We have used $\eta = 0.1$ MeV, less than 5% of the deuteron binding energy in free space. The Fermi-motion integral is performed following an adaptive trapezoidal quadrature to ensure convergence.

3. Results

Self-consistent solutions for $U(k)$ were obtained in the range $0 < k_F \leq 1.75$ fm^{-1} using the Argonne v_{18} bare internucleon potential [9]. We have included all *NN* partial waves up to $J = 7$, the total angular momentum. This criterion was maintained at all densities in order to cross-check our findings near the saturation point and to rule out any subtle variation of the calculated observables as caused by a discrete (sudden) change of in the number of partial waves. With these specifications, each cycle at which U is calculated may involve of the order of half a million matrix inversion operations.

Different strategies were followed in searches for the self-consistent solutions for the cases $0 < k_F < 0.35$ fm^{-1} and $k_F \geq 0.35$ fm^{-1}. In the second case, we calculated the solutions at Fermi momenta $k_F = 0.35(0.05)1.75$ fm^{-1}, obtaining unique stable self-consistent solutions. In contrast, searches in the range $0 < k_F < 0.35$ fm^{-1}, required a specific strategy due to the fact that two different self-consistent solutions are found for the same value of k_F. These two solutions, meeting self-consistency criteria, shall be referred to as *coexisting solutions*. To proceed systematically, a first class of solutions was obtained with ascending k_F, in steps of $\Delta k_F = 0.01$ fm^{-1}. At each k_F, the self-consistent loop starts with an $U(k)$ borrowed from the converged solution at the previous k_F. This way, starting at $k_F = 0.01$ fm^{-1}, we obtain a class of self-consistent solutions characterized by a monotonically increasing binding energy per nucleon, B/A, as a function of k_F. This class of solutions is denoted as $U_I = \{U_{k_F} \,|\, 0 \leq k_F \leq k_\beta\}$, with k_β the maximum (critical) Fermi momentum at which self-consistency is achievable in ascending order. To resolve k_β, self-consistent solutions were explored with increasing k_F in steps Δk_F as small as 0.001 fm^{-1}, obtaining $k_\beta = 0.285$ fm^{-1}. Beyond this point the iteration loops indefinitely, with fluctuations in $U(k)$ unable to settle below 0.04 MeV, the maximum fluctuation required for convergence. A more refined characterization of the solutions near and beyond k_β may require a more specific approach. A similar procedure was adopted for decreasing k_F, starting from the converged solution at $k_F = 0.35$ fm^{-1} and going down in steps of 0.01 fm^{-1}. As in the previous case, the continuity of B/A is monitored and we seek the minimum critical value of k_F, denoted by k_α, at which self-consistency is reachable with decreasing k_F. This second class of solutions is denoted $U_{II} = \{U_{k_F} \,|\, k_F \geq k_\alpha\}$. For these solutions we have found $k_\alpha = 0.130$ fm^{-1}, with a resolution of 0.01 fm^{-1}.

In Fig. 1 we show surface plots for the self-consistent fields $U(k)$ for solutions I and II in the range 0.05 fm$^{-1} \leq k_F \leq 0.35$ fm^{-1}. These solutions define distinct surfaces at densities corresponding to $k_\alpha \leq k_F \leq k_\beta$. The upper sheet, representing U_I, features a moderate repulsion at $k = 0$, with a shallow ditch in the vicinity $k \sim 4k_F/3$. On the other hand the sheet for U_{II} starts with negative mean fields at $k = 0$, showing a moderate decrease up to $k \sim k_F$ and then followed by a steep increase to reach $U(k) \to 0$. In both cases the slope of the self-consistent fields become negative at the Fermi surface, a feature that causes nucleon effective masses to be greater than the bare nucleon mass. Here we evaluate

$$\frac{m^*}{m} = \left[1 + \frac{m}{k}\frac{\partial U(k)}{\partial k}\right]^{-1}, \tag{3.1}$$

at $k = k_F$.

In Fig. 2 we plot the ratio m^*/m as function of k_F for the two solutions. Dark and light diamonds denote U_I and U_{II}, respectively. We note that in the coexistence range the unbound
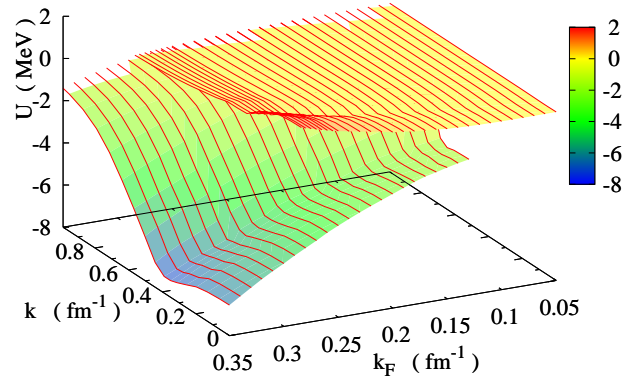
Figure 1: Self-consistent solutions at zero temperature for $U(k)$ as function of of k and k_F. The upper sheet represents U_I and the lower one corresponds to U_{II}.
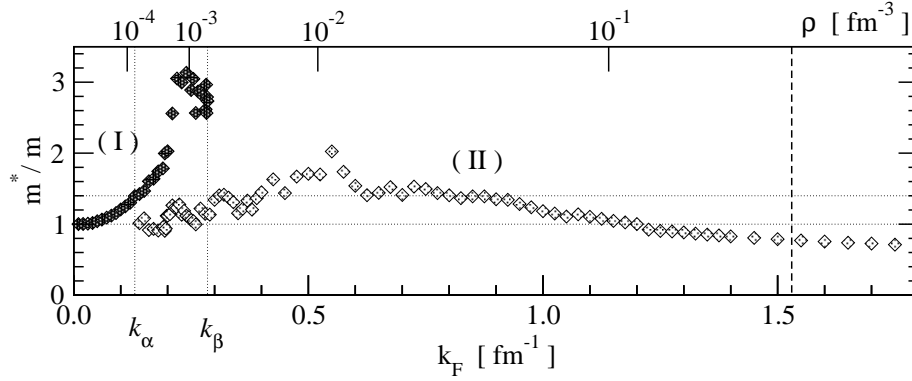

Figure 2: Effective mass m^*/m as function of k_F for solutions I and II.

solutions I yield effective masses as high as 3, consistent with the structure of the solutions for $k \sim k_F$, in resemblance to Heavy Fermions in strongly correlated systems [10].

In Fig. 3 we plot the binding energy per nucleon for symmetric nuclear matter, B_I/A and B_{II}/A, as obtained from solutions U_I and U_{II}, respectively. Here each small dot denotes an actual calculation, while the continuous curves represent suitable parametrizations. We note that the two solutions exhibit distinct behaviors as functions of k_F in their respective domains, without intercepting each other in the range $[k_\alpha, k_\beta]$. While solution I resembles a correlated Fermi gas (FG) in a metastable state, solution II represents a condensed medium featuring a minimum at the point of nuclear saturation. From the inset for low densities we also note that solution I departs from an uncorrelated FG above k_α, the Fermi momentum where solution II begins. This departure features a moderate repulsiveness relative to a free FG.

We have also investigated the occurence of dinucleon bound states at finite temperature. In this case we follow a naive extension of the BHF approach, where the density of states at a given
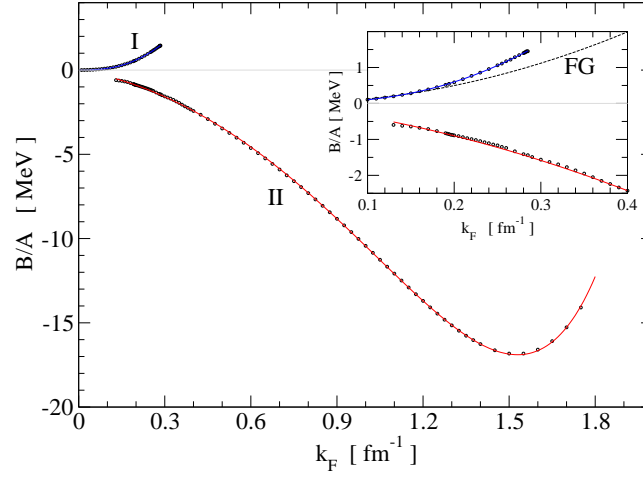
Figure 3: Calculated binding energy per nucleon B/A for symmetric nuclear matter as a function of the Fermi momentum k_F. The solid blue (red) curve corresponds to solution I (II) based on power fits. Small circles denote results from actual self-consistent runs. The inset shows a close up for the coexisting solutions together with the Fermi gas result.

momentum k is given by

$$n(k) = \Theta(e_F - e_k) \rightarrow \frac{1}{1 + e^{(e_k - \mu)/T}}, \tag{3.2}$$

with e_F the Fermi energy and μ the chemical potential [11]. The latter is found self-consistently by imposing

$$\rho = 2 \int \frac{d^3k}{(2\pi)^3} n(k), \tag{3.3}$$

to match the density of nucleons. Additionally, the Pauli blocking operator in Eq. (2.1) is modified accordingly

$$Q = \Theta(k_1 - k_F)\Theta(k_2 - k_F) \rightarrow [1 - n(k_1)][1 - n(k_2)]. \tag{3.4}$$

All other numerical procedures used in this case are the same as in the case of zero temperature. Results for the self-consistent solutions are shown in Fig. 4. The application here is for $kT = 0.2$ MeV, displaying also coexisting solutions for k_F above 0.2 fm^{-1}. Eventually, finite temperature calculations will provide us with a critical temperature, above which coexistence breaks down. Our current estimates suggest this is below 1 MeV. We note that the calculations we report in this work are computationally very intensive, and the strategy of reaching convergence to generate solutions in ascending/descending k_F prevents us from resorting to parallel runs.

4. Concluding remarks

We have investigated dinucleon formation in homogeneous symmetric nuclear matter at $T = 0$ and $T > 0$. In this work it has been crucial to treat the sp solutions $U(k)$ without resorting to the effective-mass approximation, a consideration which has led us to identify coexisting self-consistent sp fields in the range $0.13 \le k_F \le 0.285$ fm^{-1}. Work in progress also suggests coexisting
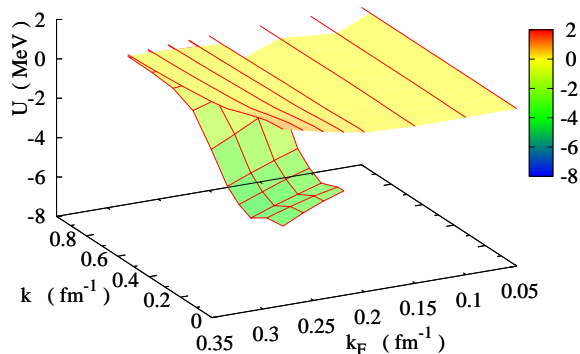
Figure 4: Self-consistent sp fields as function of k and k_F at finite temperature ($kT = 0.2$ MeV).

solutions at finite temperature, but further research is needed to pin down the temperature at which coexistence disappears. Although not discussed above, studies at zero temperature for the particle-particle wavefunctions yield bound states with sizes much greater than the internucleon distance, stressing the importance of long-range correlations. This fact has been inferred from the evaluation of mean radii, which can reach values as large as ~ 100 fm. A more detailed report of these findings shall be published elsewhere.

Acknowledgments

References

[1] W. H. Dickhoff and D. Van Neck, *Many-Body Theory Exposed!* (World Scientific, Singapore, 2008).

[2] M. Baldo (Ed.), in *Nuclear Methods and the Nuclear Equation of State*, International Review of Nuclear Physics, Vol. 8 (World Scientific, Singapore, 1999).

[3] H. F. Arellano and E. Bauge, Phys. Rev. C **84**, 034606 (2011).

[4] K. Amos, P. J. Dortmans, H. V. von Geramb, S. Karataglidis, and J. Raynal, in *Advances in Nuclear Physics*, Vol. 25, edited by J. W. Negele and E. Vogt (Plenum, New York, 2000).

[5] S. Typel, G. Röpke, T. Klähn, D. Blaschke, and H. H. Wolter, Phys. Rev. C **81**, 015803 (2010).

[6] B. E. Vonderfecht, C. C. Gearhart, W. H. Dickhoff, A. Polls and A. Ramos, Phys. Lett. B **253**, 1 (1991).

[7] A. Ramos, A. Polls and W. H. Dickhoff, Nucl. Phys. A **503**, 1 (1989).

[8] S. Heckel, P. P. Schneider, and A. Sedrakian, Phys. Rev. C **80**, 015805 (2009).

[9] R. B. Wiringa, V. G. J. Stoks, and R. Schiavilla, Phys. Rev. C **51**, 38 (1995).

[10] H. v. Lohneysen, A. Rosch, M. Vojta, and P. Wolfle, Rev. Mod. Phys. **79**, 1015 (2007).

[11] M. Baldo and L. Ferreira, Phys. Rev. C **59**, 682 (1999).